S1 Drifting collar identification

Collars deployed since 2011 were equipped with 'activity sensors' that are triggered following an extended period of inactivity. These collars were considered passively drifting if the activity sensor turned on and stayed until the end of transmissions. For collars deployed before 2011 had to be identified manually in two stages.

First, GPS location data were annotated with sea ice motion vectors from NSIDC's Polar Pathfinder Daily 25 km EASE-Grid Sea Ice Motion Vectors, Version 3 (http://nsidc.org/data/nsidc-0116). Daily drift estimates were spatiotemporally interpolated to match the location and time of GPS fixes - it was assumed that the ice motion data reflected average drift at noon of each day. For all 4 h GPS fixes, voluntary bear movement was estimated by subtracting the component of ice drift from the GPS displacement. This estimate of voluntary movement was plotted against time for each collar. Collars were suspected to be drifting if there was a sudden and sustained drop in movement speed (e.g., Figure S1 versus Figure S2). To confirm that the collars are indeed drifting, the displacement of these suspect collars had to be confirmed to reflect the actual sea ice drift.
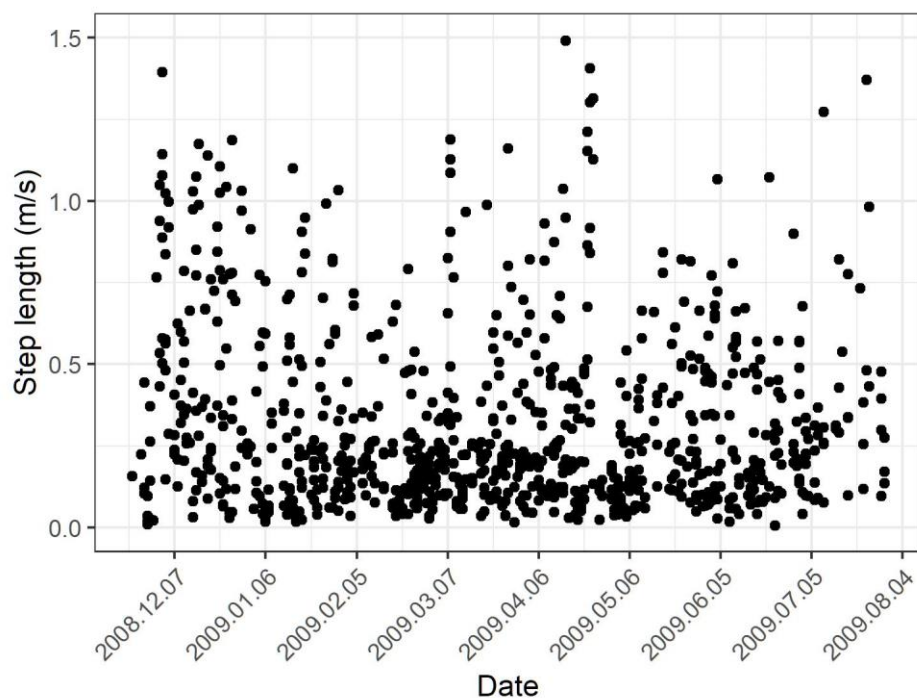
Figure S1. Example of estimated voluntary movement (step length in m s^{-1}) over time of a collar that is on a living bear.
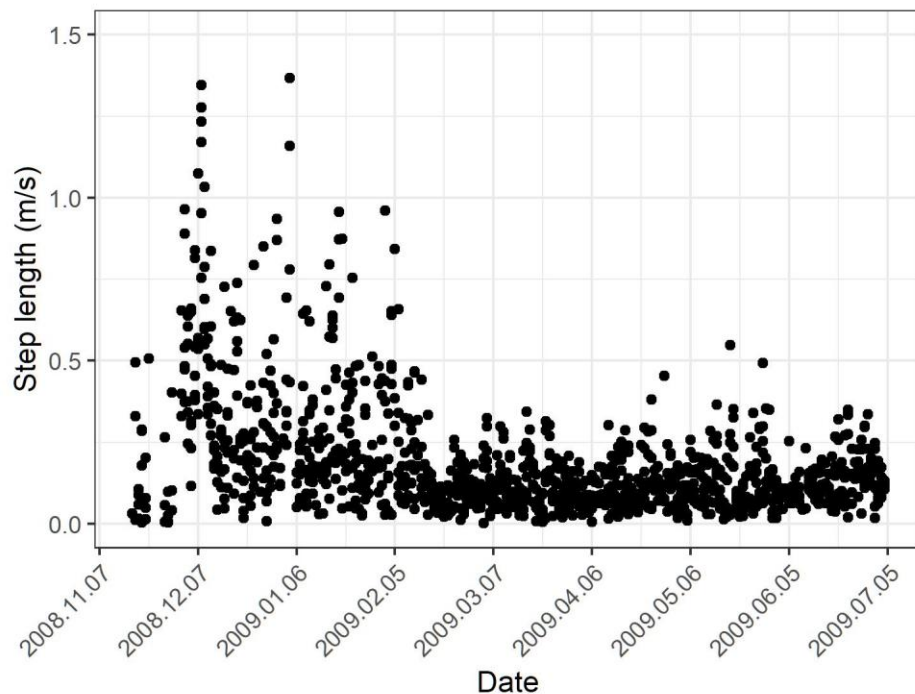
Figure S2. Example of estimated voluntary movement (step length in m s⁻¹) over time of a suspect passive collar.

Actual sea ice drift was derived from NASA's Earth Observing System Data and Information System (EOSDIS) satellite imagery (https://earthdata.nasa.gov/about). First, the projection and scale of EOSDIS and collar locations had to be matched. EOSDIS Worldview web interface (https://worldview.earthdata.nasa.gov/) projection was set to "Arctic" (WGS 84 / NSIDC Sea Ice Polar Stereographic North projection; EPSG: 3413), rotated -69°, and was maximally zoomed in. Collar locations were plotted in QGIS Version 2.16.3, the projection was matched to EOSDIS (EPSG: 3413) and scaled in QGIS to 1:480,000 (though the realized scale was ~ 1:1,330,000 on the 13.3 inch computer at a 2560×1600 resolution).

Next, sea ice drift was estimated at a subset of locations for each suspected drifting collar using the following procedure. First, the view in QGIS was centred on GPS locations of a probably drifting collar where ice drift would be approximated and the view in EOSDIS Worldview was matched. Second, we identified periods where the satellite imagery was relatively unobscured by clouds for at least two days and visually tracking ice floes would be possible. Third, a collar location representing the first location of a displacement vector (hereafter, first-day collar location) was marked using the screen annotation software AnnotatePro (http://www.annotatepro.com/). Fourth, we identified unique sea ice features that could be tracked over both days. Unique ice features were mainly distinctive edges and corners of ice floes and fractures. Fifth, using AnnotatePro, we marked where an ice floe was on the day of the collar location (hereafter, first-day ice location) and another point was marked where that same ice floe was on the following day (hereafter, second-day ice location). Sixth, both marks were selected using selection tool in AnnotatePro and moved such that the first-day ice location overlapped the first-day collar location. The second-day ice location represented where the collar would be located on the following day had the bear not moved. If the collar location was on an identified ice floe, only that floe was tracked. If the collar location was not on an identified floe, up to five

additional floes around the collar location were identified and marked to attain an approximation of drift at the collar location. Seventh, the distance between second-day ice location and the second-day collar location was calculated using the 'measure line' tool in QGIS. If several ice floes were marked and tracked, then the distance was measured from the second-day collar location to the approximate centre of all the second-day ice floe locations. At the operating scale being used, sea ice drift was relatively uniform and there was very high consistency in drift among ice floes.

Collars were assumed to be passively drifting collars if the mean of at least four consecutive distance estimates (hereafter, distance estimate) was < 2 km (hereafter, distance threshold). At the maximum resolution permitted in EOSDIS, the 2 km distance threshold corresponded to ~ 1.5 mm on screen. If the distance estimate was greater than the distance threshold, the collar was assumed to be on a live bear and not a drifting collar.

The EOSDIS imagery used was taken during daylight hours, so sea ice drift was estimated (as much as possible) for collar locations at 17:00 and 21:00 UTC, generally corresponding to midday in Hudson Bay. For each suspect drifting collar, sea ice drift was first estimated for the last days of collar locations; if the distance estimate was greater than the distance threshold (i.e. indicating a live bear), all prior locations must also have been on a live bear. If the distance estimates were less than the distance threshold the collar was assumed to be drifting, then drift was estimated iteratively ~ 30 d into the past until the distance estimate indicated a live bear. Next, from the last date assumed to be drifting, sea ice drift was estimated iteratively ~ 7 d into the past until the mean distance estimate indicated a live bear. Finally, from the last drifting collar date, I examined prior days sequentially until the distance estimate indicated a live bear. The following day was determined to be the date when the collar either dropped off the bear or the bear died.

For certain days, ice drift estimation was either very poor or not possible. Confounding factors included: heavy cloud cover, blurry satellite imagery, small floes that were indistinguishable and not trackable (particularly common during freeze-up and break-up), consolidated ice with no trackable features, or days with extreme fracturing of ice floes beyond recognition. For these periods, certain modifications to the described protocols were permitted. For example, if cloud-free days were separated by up to two clouded days and sea ice drift could be estimated across that period, this was permitted. If many of the drift estimates were poor, researcher discrepancy was permitted to increase the drifting collar threshold from 2 km. During periods with extensively poor ice drift estimation, if four sequential drift estimates spanned beyond a week, it was permitted to average fewer than four estimates.

S2 Drifting collar validation

To lend additional support that manually identified collars were indeed not on active bears, we compared metrics of speed, direction, and u/v component accuracy calculated for manually identified collars, activity sensor identified collars, and active collars. First, we subset the active collars to a 24 h resolution by filtering only fixes obtained at 13:00 UTC. Second, calculated the displacement vectors (speed, direction, and u/v components; calculated in the EASE-Grid North projection, EPSG: 3408) between successive days, then we filtered any vectors representing displacement over > 24 h. Third, we subset the active collar vector data to the same number of locations as the drifting collars (n = 1677) and only in the years (2005, 2008-2010, and 2013-2015) and months (December-June). These data were then compared to drifting collars identified manually and using the activity sensor.

The metrics of comparison were speed accuracy ($Speed_{NSIDC} - Speed_{collar}$; Figure S3 (a)), direction accuracy ($Direction_{NSIDC} - Direction_{collar}$; Figure S3 (b)). We also tested the correlation in speed, direction, u component, and v component between NSIDC drift estimates and collar displacement vectors (Figure S3 C and Figure S4). For speed, we calculated the Pearson's correlation coefficient (Figure S3 (c)). For direction, we calculated the circular Pearson's correlation coefficient ($\pm$ 95% CI) using the 'cor.circular' function in the 'circular' package in R. We used bootstrapping with 1000 replicates to calculate 95% CI for this circular correlation (Figure S3 (c)). As an additional metric of directional accuracy, we estimated the concentration parameter (kappa $\pm$ 95% CI) on the difference between NSIDC drift and collar displacement vectors (Figure S3 (c)). Last, we fit a GLMMPQL (family: Gaussian) with the NSIDC drift u and v components as functions of u and v components of active, manually identified, and activity sensor identified collars (Figure S4).

There were no significant differences between manually identified drifting collars (n = 13) and collars identified using activity sensor (n = 7) in accuracy metrics of speed, directional, or u and v components. However, both manually and activity sensor identified collars were consistently significantly different from collars on active bears with regard to the same accuracy metrics (Figure S3 and Figure S4). All results exhibit a significantly weaker relationship between NSIDC drift and displacement of active collars compared to either passively drifting collars.

The motion for six manually identified collars is depicted in the supplement video (http://doi.org/10.5446/45186). This video depicts the large degree of concurrence of drift vectors across large spatial extent, and further lends evidence that the manually identified collars are in fact passively drifting.
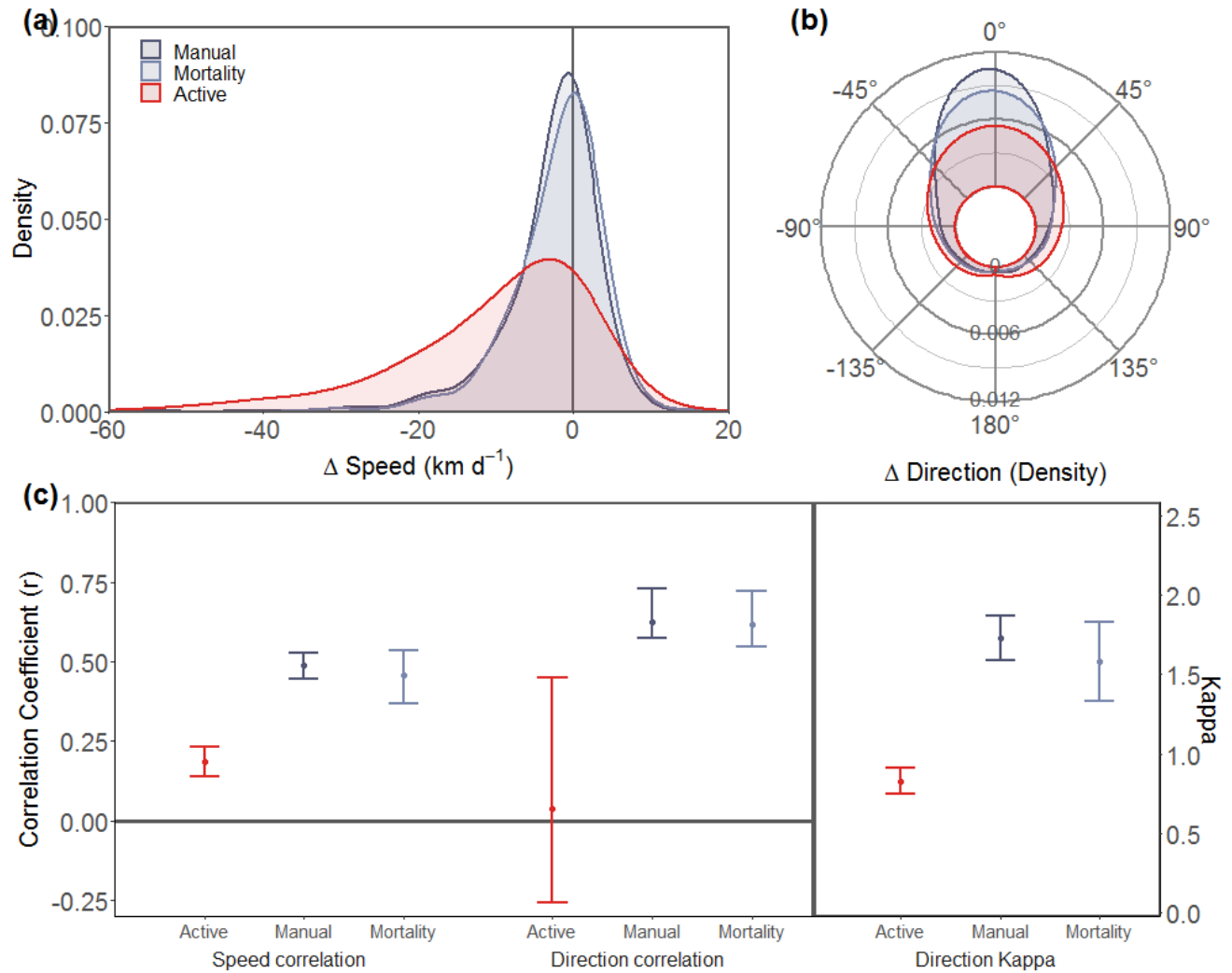
Figure S3. Comparison of speed and direction metrics of collars believed to be on active bears (red), manually identified drifting collars (dark blue), and 'activitysensor' identified drifting collars (light blue). Metrics presented are density plot of the difference in speed, ($Speed_{NSIDC} - Speed_{collar}$; A), density plot of difference in direction ($Direction_{NSIDC} - Direction_{collar}$; B), Pearson's correlation coefficients of speed ($Speed_{NSIDC} \sim Speed_{collar}$; C, left) and direction ($Direction_{NSIDC} \sim Direction_{collar}$; C, middle), and estimated of angular concentration (kappa) in the difference in direction (C, right). Error bars in C represent 95% CI of the mean.
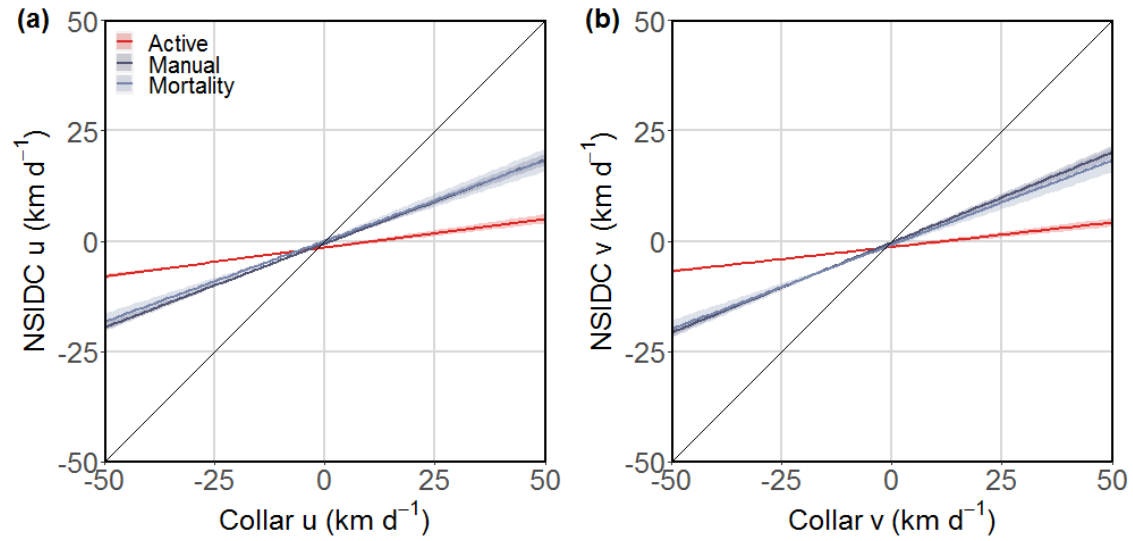
Figure S4. GLMM$_{PQL}$ regression of the u (A) and v (B) components of NSIDC drift vector versus collar drift among collars believed to be on active bears (red), manually identified drifting collars (dark blue), and 'activity sensor' identified drifting collars (light blue). Black lines represent a 1:1 relationship between NSIDC and collar drift components; Shaded areas representing 95% CI of the mean.